PRAMANA — journal of physics

Vol. 85, No. 1
July 2015
pp. 105–114

# Measurements of egg shell plasma parameters using laser-induced breakdown spectroscopy

WENFENG LUO[1,*], XIAOXIA ZHAO[2], SHUYUAN LV[1] and HAIYAN ZHU[1]

[1]School of Electronic Engineering, Xi'an University of Posts and Telecommunications, Xi'an, Shaanxi 710121, China
[2]School of Physics and Mechanical and Electronic Engineering, Xi'an University, Xi'an, Shaanxi 710065, China
*Corresponding author. E-mail: luowenfeng@xupt.edu.cn

MS received 13 July 2013; revised 23 April 2014; accepted 11 June 2014
**DOI:** 10.1007/s12043-014-0893-4; ***e*Publication:** 23 January 2015

**Abstract.** Measurements of 1064 nm laser-induced egg shell plasma parameters are presented in this paper. Of special interests were its elemental identification and the determination of spectroscopic temperature and electron density. The electron temperature of 5956 K was inferred using an improved iterative Boltzmann plot method with six calcium atomic emission lines, and the electron number density of $6.1 \times 10^{16}\,\mathrm{cm}^{-3}$ was determined by measuring the width of Stark-broadened once-ionized calcium line at 393.37 nm. Based on the experimental results, the laser-induced egg shell plasma was verified to be optically thin and satisfy local thermodynamic equilibrium (LTE). Furthermore, experiments also demonstrated that the loss of energy due to the reflection of the laser beam from the plasma can be neglected and the inverse bremsstrahlung (IB) absorption was the dominant mechanism of plasma heating at the IR wavelength.

**Keywords.** Atomic emission spectroscopy; laser-induced breakdown spectroscopy, plasma; electron temperature; electron density.

**PACS Nos 32.30.−r; 32.70.−n; 52.25.−b**

## 1. Introduction

Laser-induced breakdown spectroscopy (LIBS), a superior elemental analysis method of atomic emission spectroscopy (AES), has evolved rapidly over the past two decades [1,2]. In LIBS, a high-intensity laser is focussed onto the sample, which is strong enough to result in plasma formation through vapourization, atomization, and ionization in a single pulse [3–6]. Compared to conventional AES-based analytical methods, LIBS has many distinct advantages, including [3] short measurement times, simplicity, allows *in situ* analysis, no prior sample preparation, and simultaneous multielement detection.

Compared to the production of plasma, qualitative and quantitative analyses are not insignificant because the spectral emission intensity in the laser-induced plasma is determined not only by the concentration of the element in the sample, but also by the properties of the laser (pulse energy, wavelength, etc.), the sample and the surrounding gas [7]. Furthermore, the laser ablation processes (dissociation, atomization, ionization, and excitation) also influence the amount of the ablated mass, which in turn depend on the characteristics of the plasma (electron temperature and electron density). So, knowing these properties is beneficial for achieving accurate qualitative and quantitative analyses [4,8].

Recently, some applications of LIBS technique have been proposed in the fields of environmental monitoring, steel industry, biomedical studies, art conservation, and even in space exploration [9–12]. Though the LIBS technique has been used to assess the elements in biological samples [13,14], the application of LIBS to study egg shell is not reported yet.

In this paper, the elemental composition of the egg shell crushed to a size of about $1 \times 1$ cm was identified, and the electron density and electron temperature of laser-induced egg shell plasma were also reported. With the experimental results, the models of the plasma (local thermodynamic equilibrium and optically thin) were verified, and some other plasma parameters (plasma frequency, inverse bremsstrahlung coefficient, etc.) were calculated as well.

## 2. Experimental set-up

The schematic diagram of the experimental system used for LIBS experiments performed under atmospheric conditions is depicted in figure 1. It consists of a laser, a spectrometer with in-built charge-coupled device (CCD), and a computer for control and data acquisition. A Q-switched Nd:YAG laser (SGR, Beamtech Optronics) delivers a pulse energy of

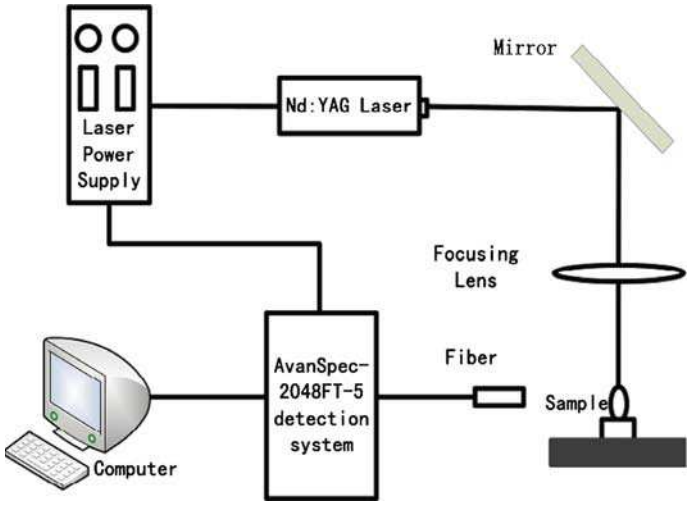


**Figure 1.** LIBS set-up for experiments.

117 mJ at the fundamental wavelength of 1064 nm and produces a 19.7 ns duration pulse at a repetition frequency of 1 Hz. The pulsed laser beam is focussed to a spot of about 200 $\mu$m in radius (OLYMPUS BX51) on the egg shell by using a 150 mm focal length lens.

Plasma emissions were collected at the right angle to the direction of the plasma expansion through a broadband spectrometer AvanSpec-2048FT-5 (Avantes, Holland, 200–720 nm range, 0.06–0.08 optical resolution with 2400–1800 grooves/mm). One end (200 $\mu$m in diameter) of the fibre bundle was used to collect the light, and its other five ends were connected to the entrance slits (10 $\mu$m in diameter) of the spectrometer. The corresponding Q-switch output of the laser was served as the external hardware trigger for the spectrometer to perform a single scan at the rising edge of transistor–transistor logic (TTL) pulse.

In order to keep the signal relatively stable, an XYZ translation stage was used and the lens-to-sample distance was a little less than the focal length. Emissions from ten laser pulses were averaged with background subtracted through AvaSoft-LIBS software and stored in a personal computer for subsequent analysis. At the same time, a delay time (5 $\mu$s) between the laser shot and the initiation of data acquisition was chosen in our experiment to obtain a good compromise between the signal background ratio (SBR) and the line emission intensity. All the experiments were performed at room temperature in air at atmospheric pressure and the sample was a normal egg shell collected in Xi'an, China.

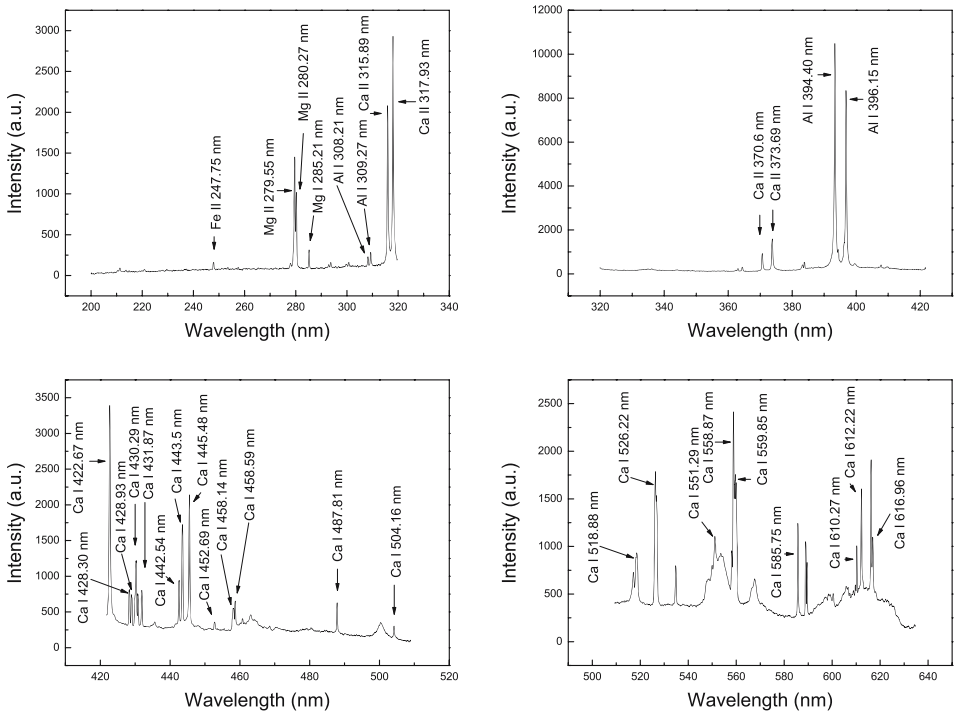


**Figure 2.** Segments of emission spectra of laser-induced egg shell plasma.

## 3. Results and discussion

### 3.1 *Description of plasma emission*

Figure 2 shows the emission spectra averaged with ten single spectrum of laser-induced egg shell plasma in air in the 200–620 nm range. As can be seen in the figure, a typical spectrum is characterized by atomic, ionic emission lines and by continuum emission. At the beginning, after the plasma formation, the light emission is dominated by the continuum emission, which is caused by recombination radiation (free-bound) and bremsstrahlung emission (free-free) [6]. As time passes, the continuum emissions decrease dramatically, and ionic and atomic emissions begin to increase.

Based on NIST database [15], several representative emission lines belonging to iron, magnesium, aluminum, and calcium elements were identified and are shown by arrows in figure 2. Six calcium atomic emission lines were used to calculate the plasma temperature and the electron density of the egg shell plasma was inferred using the once-ionized calcium emission line at 393.37 nm. The corresponding parameters of the lines are presented in table 1.

### 3.2 *Determination of excitation temperature*

Plasma characteristics such as excitation temperature and electron density are vital for understanding the processes that govern laser ablation. In laser-induced plasmas, the

**Table 1.** Physical parameters for Ca I and Ca II transitions used in our experiments.

| Species | Wavelength (nm) | $E_m$ ($cm^{-1}$) | $E_n$ ($cm^{-1}$) | $A_{mn}(10^7\ s^{-1})$ | $g_m$ | $g_n$ |
|---|---|---|---|---|---|---|
| Ca I | 428.30 | 38551 | 15210 | 4.34 | 5 | 3 |
| Ca I | 428.93 | 38464 | 15157 | 6 | 3 | 1 |
| Ca I | 430.25 | 38551 | 15315 | 13.6 | 5 | 5 |
| Ca I | 431.87 | 38464 | 15315 | 7.40 | 3 | 5 |
| Ca I | 442.54 | 37748 | 15157 | 4.98 | 3 | 1 |
| Ca I | 443.5 | 37751 | 15210 | 6.70 | 5 | 3 |
| Ca I | 445.48 | 37757 | 15315 | 8.70 | 7 | 5 |
| Ca I | 452.69 | 43933 | 21849 | 4.10 | 3 | 5 |
| Ca I | 458.14 | 42170 | 20349 | 2.10 | 7 | 5 |
| Ca I | 458.59 | 42171 | 20371 | 2.30 | 9 | 7 |
| Ca I | 487.81 | 42343 | 21849 | 1.88 | 7 | 5 |
| Ca I | 504.16 | 41679 | 21849 | 3.30 | 3 | 5 |
| Ca I | 518.88 | 42919 | 23652 | 4 | 5 | 3 |
| Ca I | 526.22 | 39333 | 20335 | 6 | 1 | 3 |
| Ca I | 551.29 | 41786 | 23652 | 11 | 1 | 3 |
| Ca I | 558.87 | 38259 | 20371 | 4.90 | 7 | 7 |
| Ca I | 559.85 | 38192 | 20335 | 4.30 | 3 | 3 |
| Ca I | 585.75 | 40719 | 23652 | 6.60 | 5 | 3 |
| Ca I | 610.27 | 31539 | 15157 | 0.96 | 3 | 1 |
| Ca I | 612.22 | 31539 | 15210 | 2.87 | 3 | 3 |
| Ca I | 616.96 | 36575 | 20371 | 1.90 | 5 | 7 |
| Ca II | 393.37 | 25414 | 0 | 14.70 | 4 | 2 |

kinetic, excitation, ionization, and radiative energies of the system are described by the Maxwell, Boltzmann, Saha, and Planck functions, respectively [5]. However, when electron collision dominates, the state of the typical LIBS plasma can be described by local thermodynamic equilibrium, and the single plasma electronic excitation temperature $T_e$ satisfies the Boltzmann, Saha, and Maxwell distributions. In this state, the population of the excited levels for each species obeys the Boltzmann distribution [16]:

$$\ln\left(\frac{\lambda_{mn} I_{mn}}{h c g_m A_{mn}}\right) = -\frac{E_m}{k T_{\mathrm{e}}} + \ln\left(\frac{N(T)}{U(T)}\right), \tag{1}$$

where $A_{mn}$ is the transition probability, $\lambda_{mn}$ is the wavelength, $h$ is the Plank's constant, $g_m$ is the statistical weight of the upper level, $c$ is the speed of light in vacuum, $E_m$ is the upper level energy, $k$ is the Boltzmann constant, $T_{\mathrm{e}}$ is the electron temperature, $U(T)$ is the partition function, and $N(T)$ is the total number density of the species. A plot of the left-hand side of the equation vs. $E_m$ has a slope of $-1/(kT_{\mathrm{e}})$. Therefore, the plasma temperature can be inferred using linear regression.

A series of lines from different excitation states of the same species instead of just a pair usually lead to greater precision of the plasma temperature evaluation. However, the transition probability values given in the literature exhibit significant degrees of uncertainty (from 5 to 50%) [5]. To minimize the uncertainty in determining egg shell temperature, an improved iterative Boltzmann plot method was used in [17]. First, 21 Ca I emission lines were selected as potential candidates for calculating the temperature as shown in figure 3. Apparently, when all the measured calcium lines were used for calculating the temperature, a rather scattered Boltzmann plot was obtained leading to an unreliable plasma temperature value. In order to reduce the scatter, the distance of each datum to the fitting line was calculated and the datum with the maximum distance was discarded. Then, the regression function was recalculated with the remaining data until the threshold value of 0.99 was reached. After 15 iterations, plasma temperature of 5956 K with a better

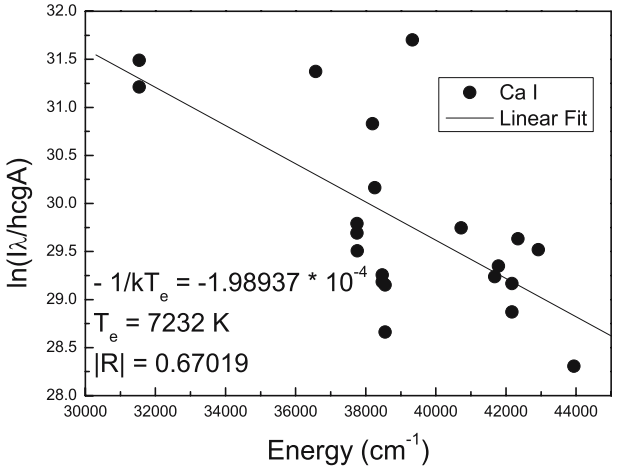


**Figure 3.** Boltzmann plot with 21 Ca I emission lines in laser-induced egg shell plasma. The fitting correlation coefficient $R = 0.67019$.

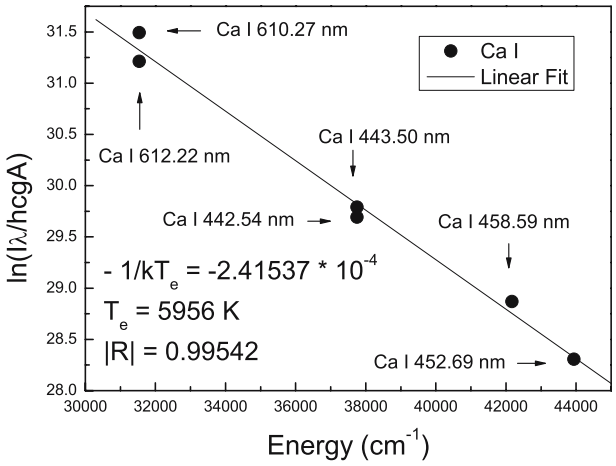


**Figure 4.** Boltzmann plot with six Ca I emission lines in laser-induced egg shell plasma. *R* increases to 0.99542 after 15 iterations.

regression coefficient of 0.99542 was obtained which is shown in figure 4, and the corresponding parameters of the calcium lines are presented in table 1 as well. Similarly, figure 5 also depicts the variations of $R$ and $T_e$ with the iterations. The experiments showed that with the scatter removed, the accuracy and precision of the measurements were substantially improved.

### 3.3 *Determination of electron density*

The plasma electron density can be obtained using the spectroscopic method, which requires measuring the Stark broadening of plasma lines [5]. In laser-induced plasma,

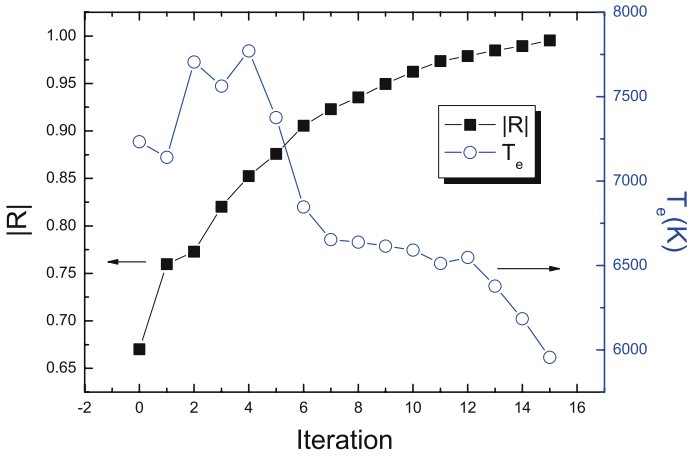


**Figure 5.** Variations of correlation coefficient and plasma temperature vs. the iteration for Ca I emission lines in laser-induced egg shell plasma.

the dominant broadening mechanism of the line profile is [18]. The full-width at half-maximum intensity (FWHM) of the Stark broadening is related to the electron density by the expression [19]

$$\Delta\lambda_{1/2} = 2w\left(\frac{N_e}{10^{16}}\right) + 3.5A\left(\frac{N_e}{10^{16}}\right)^{1/4} \times [1 - 1.2N_D^{-1/3}] \times w\left(\frac{N_e}{10^{16}}\right), \quad (2)$$

where $\Delta\lambda_{1/2}$ is the FWHM of the line, $A$ is the ion broadening parameter, $w$ represents the electron impact parameter and $N_D$ is the number of particles in the Debye sphere. For typical LIBS conditions, the contribution from ion broadening is negligible [5], and eq. (2) reduces to

$$\Delta\lambda_{1/2} = 2w\left(\frac{N_e}{10^{16}}\right). \quad (3)$$

Figure 6 shows the broadened profile of the once-ionized calcium emission line at 393.37 nm which was fitted with a Lorentzian line with a correlation coefficient of 0.995 and FWHM of 0.41 nm. With the value of the electron impact parameter [20], the electron number density was inferred to be $6.1 \times 10^{16}$ cm$^{-3}$ with instrumental line broadening subtracted.

### 3.4 *LTE requirement*

In the measurements of plasma temperature, LTE was hypothesized, which requires that the collision excitation and de-excitation processes predominate over the radiative

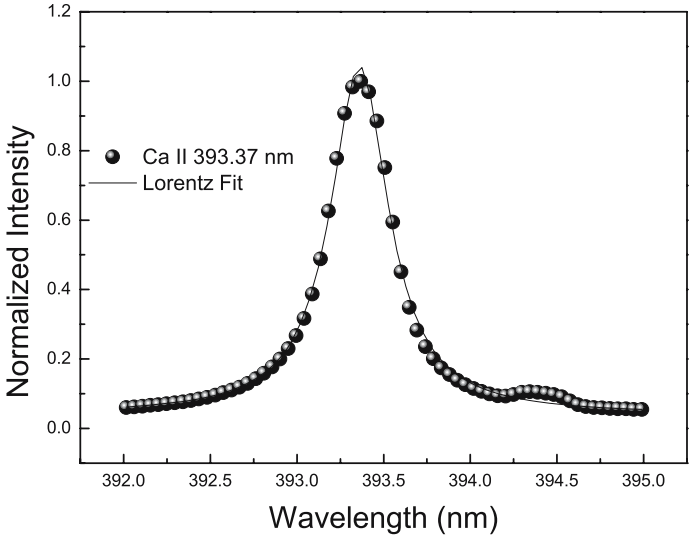


**Figure 6.** Stark-broadened profile of Ca II 393.37 nm in laser-induced egg shell plasma.

processes and a minimum electron density is required [21]. The lower limit for the electron density for which the plasma will be in LTE is [6]

$$N_e(\mathrm{cm}^{-3}) \geq 1.6 \times 10^{12} T_e^{1/2}(K)[\Delta E(\mathrm{eV})]^3, \quad (4)$$

where $\Delta E$ (eV) is the difference between the states which are expected to be in LTE, and $T_e$ is the temperature of the plasma. With the lines being used, the maximum $\Delta E$ is 3.1 eV (Ca II 393.37 nm), and the minimum electron number density should be $3.7 \times 10^{15}$ cm$^{-3}$ with the temperature obtained earlier. As the requirement limit was much lower than the electron number density obtained, the condition for LTE was fulfilled for the laser-induced egg plasma in our experiments.

### 3.5 *Self-absorption*

When the electron temperature is evaluated, the plasma should be optically thin for the lines used. This means that the radiation is not reabsorbed along the optical path between the plasma and the detector [4]. In the absence of self-absorption, the intensity ratio $(I_2/I_1)$ of two emission lines from similar species with the same upper energy level should be the same as the ratio of $(Y_2/Y_1)$, where $Y$ represents $(g_m A_{mn}/\lambda)$ according to the Boltzmann distribution [5,6,16]. Take Ca I 612.22nm, Ca I 610.27nm, Ca I 428.93nm and Ca I 431.87 nm. The observed intensity ratios of $I_{\mathrm{CaI612.22\,nm}}/I_{\mathrm{CaI610.27\,nm}}$ and $I_{\mathrm{CaI428.93\,nm}}/I_{\mathrm{CaI431.87\,nm}}$ are 2.25 and 0.87, which are approximately equal to the value 2.98 of $Y_{\mathrm{CaI612.22\,nm}}/Y_{\mathrm{CaI610.27\,nm}}$ and 0.82 of $Y_{\mathrm{CaI428.93\,nm}}/Y_{\mathrm{CaI431.87\,nm}}$ within the experimental uncertainty.

Furthermore, among the emission lines used in our experiments, no flat-topped profiles or dips at the final frequencies were found, and even the resonance line 393.37 nm was very well fitted with a Lorentzian line ($R^2 = 0.995$, figure 6). All of these indicated that the current plasma was free from self-absorption and self-reversion.

### 3.6 *Other parameters*

When a high-power nanosecond (19.7 ns in this case) laser pulse strikes a solid surface, a plume is produced initially due to rapid melting and vapourization of the sample surface [4]. The plasma plume gets elongated towards the incident laser beam as a result of laser–plasma interaction. That is to say, some of the laser energy may be transmitted through the plasma volume, some scattered, and the rest absorbed [6]. After the end of the pulse, adiabatic expansion of the plasma occurs.

The process of laser–plasma interaction depends on the electron temperature and electron density. As is known, the laser beam will be reflected when the plasma frequency becomes less than the laser photon frequency [22]. The plasma frequency is approximately $5.4 \times 10^{11}$ Hz on using the formula $\nu_p = 8.9 \times 10^3\, N_e^{0.5}$ with the electron density obtained earlier [22]. For a 1064 nm Nd:YAG laser, the corresponding laser frequency $2.82 \times 10^{14}$ Hz is much larger than the plasma frequency. So the loss of energy due to the reflection of the laser beam from the plasma is insignificant.

During the laser–plasma interaction, the plasma is heated to a high temperature ionized by the inverse bremsstrahlung (IB) process considering its $\lambda^3$ dependence. The IB absorption coefficient $\alpha_{IB}$ using free electrons is described as [23]

$$\alpha_{IB}(\mathrm{cm}^{-1}) = 1.37 \times 10^{-35} \lambda^3 N_e^2 T_e^{-1/2}, \quad (5)$$

where $\lambda$ ($\mu$m) is the wavelength of the laser photons, $T_e$ (K) is the electron temperature, and $N_e$ (cm$^{-3}$) is the electron number density. With the experimental results, the IB absorption coefficient $\alpha_{IB}$ was about $2.9 \times 10^{-6}$ cm$^{-1}$.

## 4. Conclusions

In this paper, the elemental composition of egg shell was first studied using LIBS technique. Based on its plasma spectra, iron, magnesium, aluminum, and calcium elements were identified. Using the Stark-broadened profile of the once-ionized calcium emission line at 393.37 nm, the electron number density of the egg shell plasma was calculated to be $6.1 \times 10^{16}$ cm$^{-3}$. The plasma temperature was inferred to be 5956 K using the Boltzmann plot method with Ca I lines (442.54, 443.50, 452.69, 458.59, 610.27 and 612.22 nm). With the experimental results, the laser-induced plasma was verified to satisfy the LTE and optically thin models. At the same time, experiments also demonstrated that the IB process is an efficient plasma-heating mechanism and the IB absorption coefficient $\alpha_{IB}$ is approximately $2.9 \times 10^{-6}$ cm$^{-1}$.

## Acknowledgements

Author wants to thank State Key Laboratory of Transient Optics and Photonics, Xi'an Institute of Optics and Precision Mechanics, CAS. This work is supported by Scientific Research Program Funded by Shaanxi Provincial Education Department (2013JK0607) and by General Program Funded by Youth Foundation of Xi'an University of Posts and Telecommunications (ZL2013-14). This work is also supported by the Natural Science Foundation of Shaanxi Province of China (2013JM1008) and National Natural Science Foundation of China (11304247).

## References

[1] B Kearton and Y Mattley, *Nature Photon.* **537**, 2 (2008)
[2] W F Luo, X X Zhao, Q B Sun, C X Gao, J Tang, H J Wang and W Zhao, *Pramana – J. Phys.* **945**, 74 (2010)
[3] M Jandaghi, P Parvin, M J Torkamany and J Sabbaghzadeh, *J. Phys. D: Appl. Phys.* **205301**, 42 (2009)
[4] J P Singh and S N Thakur, *Laser-induced breakdown spectroscopy* (Elsevier Science BV, Amsterdam, 2006)
[5] A W Miziolek, V Palleschi and I Schechter, *Laser-induced breakdown spectroscopy (LIBS): Fundamentals and applications* (Cambridge University Press, New York, 2006)
[6] D A Cremers and L J Radziemski, *Handbook of laser-induced breakdown spectroscopy* (John Wiley & Sons, Chichester, 2006)
[7] W F Luo, X X Zhao, H Y Zhu, D D Li and X L Li, *High Power Laser Part. Beams* **1690**, 25 (2013)
[8] X X Zhao, *High Power Laser Part. Beams* **2519**, 23 (2011)
[9] A K Knight, N L Scherbarth, D A Cremers and M J Ferris, *Appl. Spectrosc.* **331**, 54 (2000)

[10] C Pasquini, J Cortez, L M C Silva and F B Gonzaga, *J. Braz. Chem.* **463**, 18 (2007) Pasquini C, Cortez J, Silva L M C *et al*, *J. Braz. Chem. Soc.* **18**, 463 (2007)
[11] J L Wu, Y X Fu, Y Li, Y Lu, Z F Cui and E R Zheng, *Spectrosc. Spect. Anal.* **1979**, 28 (2008)
[12] S Pandhija and A K Rai, *Pramana – J. Phys.* **553**, 70 (2008)
[13] M A Kasem, R E Russo and M A Harith, *J. Anal. At. Spectrom.* **1733**, 26 (2011)
[14] A El Hussein, A K Kassem, H Ismail and M A Harith, *Talanta* **495**, 82 (2010)
[15] http://www.nist.gov/pml/data/asd.cfm
[16] C Aragon and J A Aguilera, *Spectrochim. Acta Part B* **893**, 63 (2008)
[17] U Aydin, P Roth, C D Gehlen and R Noll, *Spectrochim. Acta Part B* **1060**, 63 (2008)
[18] I B Gornushkin, L A King, B W Smith, N Omenetto and J D Winefordner, *Spectrochim. Acta Part B* **1207**, 54 (1999)
[19] G Abdellatif and H Imam, *Spectrochim. Acta Part B* **1155**, 57 (2002)
[20] N Konjevic, A Lesage, J R Fuhr and W L Wiese, *J. Phys. Chem. Ref. Data* **819**, 31 (2002)
[21] M Milan and J J Laserna, *Spectrochim. Acta Part B* **275**, 56 (2001)
[22] S S Harilal, C V Bindhu, Riju C Issac, V P N Nampoori and C P G Vallabhan, *J. Appl. Phys.* **2140**, 82 (1997)
[23] N M Shaikh, S Hafeez, B Rashid and M A Baig, *Eur. Phys. J. D* **371**, 44 (2007)